ISSN 1063-7729, Astronomy Reports, 2006, Vol. 50, No. 7, pp. 544–552. © Pleiades Publishing, Inc., 2006.
Original Russian Text © M.K. Abubekerov, E.A. Antokhina, A.M. Cherepashchuk, V.V. Shimanskii, 2006, published in Astronomicheskiĭ Zhurnal, 2006, Vol. 83, No. 7, pp. 609–619.

The Mass of the Compact Object in the Low-Mass X-ray Binary 2S 0921−630

M. K. Abubekerov[1], E. A. Antokhina[1], A. M. Cherepashchuk[1], and V. V. Shimanskii[2]

[1] *Sternberg Astronomical Institute, Universitetskiĭ pr. 13, Moscow, 119992 Russia*

[2] *Kazan State University, ul. Kremlevskaya 18, Kazan, 420008 Tatarstan, Russia*

Received October 15, 2005; in final form, February 6, 2006

Abstract—We interpret the observed radial-velocity curve of the optical star in the low-mass X-ray binary 2S 0921−630 using a Roche model, taking into account the X-ray heating of the optical star and screening of X-rays coming from the relativistic object by the accretion disk. Consequences of possible anisotropy of the X-ray radiation are considered. We obtain relations between the masses of the optical and compact (X-ray) components, m_v and m_x, for orbital inclinations $i = 60°$, 75°, and 90°. Including X-ray heating enabled us to reduce the compact object's mass by $\sim 0.5-1\,M_\odot$ compared to the case with no heating. Based on the K0III spectral type of the optical component (with a probable mass of $m_v \simeq 2.9\,M_\odot$), we concluded that $m_x \simeq 2.45-2.55\,M_\odot$ (for $i = 75°-90°$). If the K0III star has lost a substantial part of its mass as a result of mass exchange, as in the V404 Cyg and GRS 1905+105 systems, and its mass is $m_v \simeq 0.65-0.75\,M_\odot$, the compact object's mass is close to the standard mass of a neutron star, $m_x \simeq 1.4\,M_\odot$ (for $i = 75°-90°$). Thus, it is probable that the X-ray source in the 2S 0921−630 binary is an accreting neutron star.

PACS numbers : 97.80.J
DOI: 10.1134/S1063772906070043

1. INTRODUCTION

Currently, mass estimates are available for ∼30 neutron stars. The most accurate of these are the masses of radio pulsars in Hulse−Taylor binaries [1] and of the radio pulsar J0737−3039 [2]. According to these estimates, the masses of neutron stars are confined to a fairly narrow range, $1.25-1.44\,M_\odot$. Nevertheless, theoretical arguments suggesting the possible existence of massive neutron stars with $m_{\rm NS} \simeq 2-3\,M_\odot$ have accumulated.

First, theoretical computations indicate that the expected mass of a neutron star formed during the core collapse of a massive star can lie in the range $1.0-1.8\,M_\odot$ [3–5].

Second, there exist quite a few hard equations of state for neutron matter for which the Oppenheimer–Volkoff mass exceeds $1.8\,M_\odot$ [6]. We especially note in this context recently published papers on so-called "Skyrmion stars." In 1999, Ouyed and Butler [7] considered an equation of state based on the model of Skyrme [8]. A characteristic feature of neutron-star models based on Skyrme's equation is their high upper mass limit: $2.95\,M_\odot$ for nonrotating and $3.45\,M_\odot$ for rotating stars [9, 10].

Third, evolutionary computations of neutron-star masses in binary systems using the "Scenario Machine" [11] have demonstrated that there could exist binary-system evolutionary channels for which a neutron star is able to increase its mass via accretion by more than $\sim 1\,M_\odot$ [12, 13].

Because of these argumements, special interest has been attracted by the compact object in the low-mass X-ray binary 2S 0921−630 [14]. This binary X-ray system consists of a compact object and a low-mass optical star (V395 Car) [15] of spectral type K0III [16]. The binary's orbital period is $P_{\rm orb} = 9.006^{\rm d} \pm 0.007^{\rm d}$ [17]. The nature of the compact object remains unknown: the binary does not exhibit phenomena characteristic of an X-ray pulsar or type 1 X-ray burster. Partial optical and X-ray eclipses are observed for the system, testifying to a high orbital inclination: $i \simeq 70°-90°$ [16, 18].

According to Shahbaz et al. [16], if the orbital inclination is $i = 70°-90°$, the compact object's mass is $m_x = 2.0-4.3\,M_\odot$. The component-mass ratio derived from the rotational line broadening is $q = m_x/m_v = 1.12 \pm 0.18$ [16].

Jonker et al. [17] present the results of fitting an accurate radial-velocity curve. Assuming $i = 60°-90°$, the mass of the compact object was found to be $1.90 \pm 0.25\,M_\odot < m_x < 2.9 \pm 0.4\,M_\odot$ [17].

Given the strong X-ray heating, these authors applied a so-called K-correction [19] to the semi-amplitude of the radial-velocity curve in order to estimate the component-mass ratio, $q = m_x/m_v = 0.75 \pm 0.37$ [17].

The strength of the heating of the optical star's atmosphere by X-rays from the compact object ($k_x = L_x/L_v \simeq 10$) complicates fitting of the radial-velocity curve for the 2S 0921−630 system. The model of the binary system used to analyze the observed radial-velocity curve must take into account a variety of physical phenomena related to the compact object's high X-ray luminosity.

Having in mind the importance of reliable mass estimates for the compact object in the 2S 0921−630 binary, we analyzed the high-precision data of [17] using the Roche model of [20, 21], taking into account the X-ray heating of the optical star and the screening of X-rays by the accretion disk, as well as the possible anisotropy of the X-ray radiation from the accretion disk associated with a black hole.

2. OBSERVATIONAL MATERIAL

We used the spectroscopic data of [17] for our analysis. These data were acquired between December 2003 and March 2004 with the VLT (Very Large Telescope). A total of 44 spectra with exposure times of 1300 s were obtained. The width of the spectrograph's slit was 0.4″, making it possible to take spectra with high resolution (0.75 Å per pixel). The calibration uncertainty for the wavelength scale was 0.03 Å.

The spectroscopic data were obtained using two gratings, 1200R+93 and 1028z+29, which covered 5920−6520 Å and 8360−8900 Å, respectively. The analysis of the spectrograms of the optical star in the 2S 0921−630 system performed in [17] confirmed its spectral type to be K0III. The radial velocities were determined by cross-correlating the spectra taken with the 1200R+93 diffraction grating with the spectra of a standard star. Stars with spectral types between G5 and K7 whose spectra were obtained with the Keck telescope with the same resolution were used as standard stars.

We adopted the middle of the eclipse of the X-ray component by the optical star to be zero phase when plotting the radial-velocity curve. Jonker et al. [17] used their accurate radial-velocity curve to refine the binary's orbital period, which was found to be $P_{\rm orb} = 9.006^{\rm d} \pm 0.007^{\rm d}$ relative to the zero ephemeris $\mathrm{JD}_0 = 2453000.49$. The system's spatial velocity is $\gamma = 44.4 \pm 2.4$ km/s. The semiamplitude of the observed radial-velocity curve obtained using the K1V radial-velocity standard star HD 124106 is $K_v = 99.1 \pm 3.1$ km/s. The observed radial-velocity curve relative to the γ velocity is shown in Fig. 1.

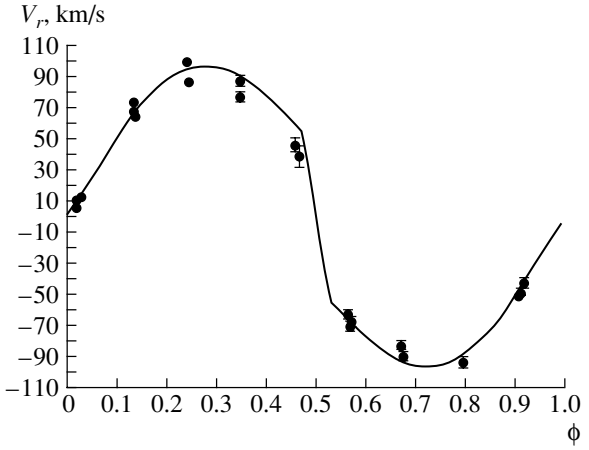

Fig. 1. Observed radial-velocity curve of the optical component of the X-ray binary 2S 0921−630 from [17] and the theoretical radial-velocity curve in the Roche model, for the compact-object mass $m_x = 2.35\,M_\odot$, optical-star mass $m_v = 2.4\,M_\odot$, X-ray heating coefficient for the optical star $k_x = 10$, and optical inclination $i = 75^\circ$ (the remaining binary parameters are collected in Table 1). The theoretical radial-velocity curve corresponds to the minimum-residual fit ($\chi^2_{\rm min} = 149.8$).

3. ANALYSIS OF THE RADIAL-VELOCITY CURVES

The optical star in the 2S 0921−630 close binary fills its Roche lobe. The star's surface is tidally and rotationally distorted, and the side facing the relativistic component is heated by X-rays from this component. These effects of the components' interaction must be taken into account when analyzing the optical component's radial-velocity curve. We fit the observed radial-velocity curve using the Roche model, taking into account the X-ray heating of the optical star. The algorithm we used is described in detail by Antokhina et al. [20−23]. We briefly summarize here the basic features of the method.

The binary consists of an optical star treated using the Roche model and a point X-ray source. The optical star's surface is subdivided into several thousand (in our case, ∼2600) area elements, for each of which we compute the emergent local flux assuming LTE, including the effect of the incident X-ray flux. Each area element is described by the local temperature $T_{\rm loc}$, local gravity $g_{\rm loc}$, and a parameter $k_x^{\rm loc}$, equal to the ratio of the incident X-ray flux to the emergent radiation flux, without taking into account external irradiation of the atmosphere. For these parameters at a given point of the surface, we solved the radiative-transport equations in a spectral line in the

Table 1. Numerical parameters used to model the optical component's radial-velocity curve in the Roche model

P, days	9.006	Orbital period
m_v, $M_\odot$	*var**	Optical star's mass
e	0.0	Eccentricity
i, deg	60, 75, 90	Orbital inclination
μ	1.0	Roche lobe filling factor for the optical component
f	1.0	Rotational asynchronism factor for the optical component
$T_{\rm eff}$, K	4700	Optical component's effective temperature
β	0.08	Gravity-darkening coefficient
k_x	*var**	Ratio of the relativistic component's X-ray luminosity to the optical component's bolometric luminosity, L_x/L_v
A	1.0	Coefficient for reprocessing of the X-ray radiation
u	0.3	Limb-darkening coefficient
$\alpha_{\rm p}$	1.2	Photon index of the X-ray spectrum

* These parameters of the X-ray binary were varied in our model fitting.

presence of the incident X-ray radiation in order to compute a model atmosphere and obtain the intensity of the emergent radiation in the line and continuum. Our model synthesis of the radial-velocity curve was performed for the CaI 6439.075 Å absorption line (hereafter, the CaI 6439 Å line). For a given phase of the orbital period, we summed the contributions of the areas to the total flux, allowing for Doppler effects and the visibility of the areas for the observer. In this way, we computed the integrated continuum radiation flux from the star towards the observer, as well as the rotation-broadened profile of the spectral line, which was used to derive the star's radial velocity. The radial velocity of the star at a given orbital phase was determined from the mean wavelengths at residual-intensity levels for the integrated absorption-line profile of one-third, one-half, and two-thirds.

We carried out our analysis both including and excluding the effect of the instrumental profile on the model integrated profile of the CaI 6439 Å line. The full width at half-maximum of the instrumental profile was taken to be FWHM = 0.5 Å. The two sets of results were virtually identical, and we accordingly present here only those including the effect of the instrumental profile on the integrated profile of the CaI 6439 Å line.

We noted above that considerable X-ray heating of the optical star's atmosphere was observed in the binary system. Thus, the X-ray spectrum must be taken into account as accurately as possible, using the known X-ray spectrum [24]. Based on observations obtained with the XMM and Chandra observatories [24], we adopted a photon index for the power-law spectrum $\alpha_{\rm p} = 1.2$ in the range 0.1–12 keV.

The compact object's intrinsic X-ray luminosity indicated by the XMM and Chandra data is $L_x \sim 10^{36}$ erg/s [24]. Assuming the mean effective temperature of the optical star filling its Roche lobe is $T_{\rm eff} = 4700$ K, its luminosity is $L_v \simeq 2 \times 10^{35}$ erg/s. Given the uncertainties in estimates of the distance to the system and of L_x, we can assume $k_x = L_x/L_v \simeq 10$. We fit the observed radial-velocity curve using the atmospheric heating coefficients $k_x = 0$ and $k_x = 10$.

We fit the observed radial-velocity curve in three different models: with screening of the X-rays by the accretion disk taken and not taken into account, and allowing for the anisotropy of the X-rays emitted by the accretion disk of a rotating black hole. The numerical parameters of the Roche model for the 2S 0921–630 binary are presented in Table 1.

Model 1. Analysis of the Observed Radial-Velocity Curve without Screening of the X-ray Flux by the Accretion Disk

Since the exact mass of the optical star is not known, we treated the masses of both binary components as parameters to be determined. Since the inverse problem is rather cumbersome in this formulation, we carried out an exhaustive search to the parameters, thereby repeatedly solving the direct problem. For each mass of the optical component m_v from the discrete set of values 1.0, 1.9, 2.4, 2.9 $M_\odot$,

Table 2. Dependence of the m_x on m_v for the Roche model including isotropic X-ray heating of the optical component with $k_x = 10$ and $i = 60°$, 75°, 90° (without screening of the X-rays by the accretion disk)

$m_v, M_\odot$	$m_x, M_\odot$		
	$i = 60°$	$i = 75°$	$i = 90°$
1.0	2.00	1.70	1.55
1.9	2.55	2.15	2.00
2.4	2.80	2.35	2.25
2.9	3.00	2.55	2.45

Table 3. Dependence of the m_x on m_v for the Roche model without heating of the optical component ($k_x = 0$) for $i = 60°$, 75°, 90°

$m_v, M_\odot$	$m_x, M_\odot$		
	$i = 60°$	$i = 75°$	$i = 90°$
1.0	2.55	2.10	1.95
1.9	3.30	2.75	2.60
2.4	3.65	3.05	2.85
2.9	4.00	3.35	3.15

fixing i, we carried out an exhaustive search for the compact object's mass m_x. We tested the model's fit to observations using the usual χ^2 statistical test, working with the significance levels $\alpha = 1$ and 5% (cf. [25] for details).

To quantitatively estimate the effect of X-ray heating on our estimates of m_x, we fit the observed radial-velocity curve with X-ray heating both taken and not taken into account, and also allowing for possible anisotropy of the X-ray radiation from inner parts of the accretion disk around a black hole. When X-ray heating was taken into account, we set $k_x = 10$. We obtained fits for inclinations $i = 60°$, 75°, and 90°. This analysis yields relations between the masses of the optical and compact objects, m_v and m_x. The numerical results are collected in Tables 2 and 3, and are plotted in Fig. 2.

Tables 2 and 3 present the values of m_x corresponding to the minimum χ^2 residuals for the difference between the theoretical and observed radial-velocity curves. The values of m_x in Tables 2 and 3 are not accompanied by uncertainties because both of the binary models were rejected at the $\alpha = 1$ and 5% significance levels. The quantiles for these significance levels are $\Delta_{1\%} = 38.93$ and $\Delta_{5\%} = 32.67$. When X-ray heating of the optical star is included ($k_x = 10$), the minimum residual is $\chi^2_{\min} \simeq 120-150$. When it is not included ($k_x = 0$), the minimum residual increases to $\chi^2_{\min} \simeq 350-380$. The statistical inadequacy of the models in describing the observational data is due to the considerable scatter of the data points, with the uncertainties in the radial velocities for each data point being comparatively small (see Fig. 4 below). As was noted in [17], the considerable

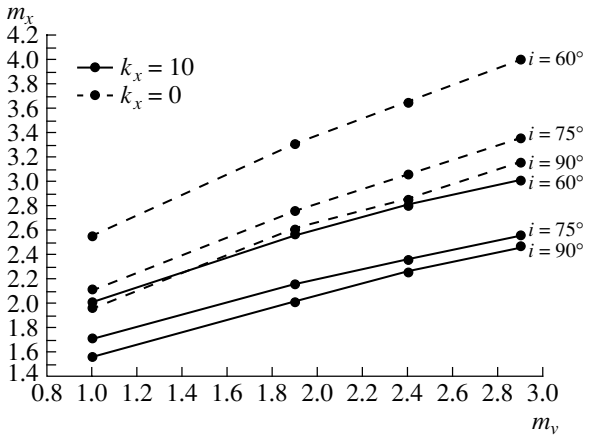

Fig. 2. Relations between the masses of the optical star and relativistic component in the 2S 0921−63 binary from our fitting of the observed radial-velocity curve using the Roche model, assuming $k_x = 10$ (solid broken lines) and $k_x = 0$ (dashed broken lines) for the X-ray heating. The X-ray heating is taken to be isotropic.

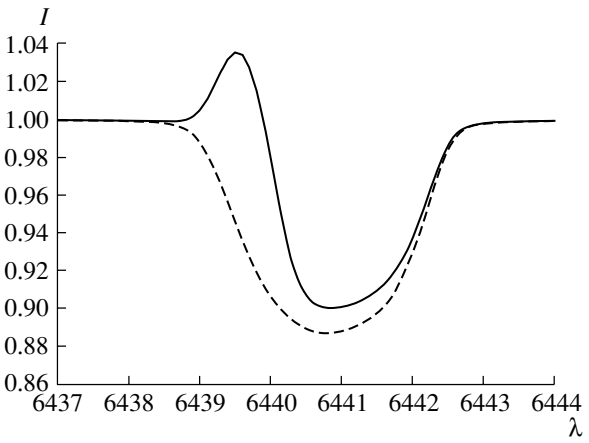

Fig. 3. Model integrated profiles of the CaI 6439 Å line of the optical component in the 2S 0921−630 X-ray binary at orbital phase 0.25. The profiles were obtained for the Roche model with $m_x = 2.35\,M_\odot$, $m_v = 2.4\,M_\odot$, and $i = 75°$. The dashed curve is the line profile derived in the Roche model without including the reflection effect. The solid curve is the line profile obtained with X-ray heating of the optical star corresponding to $k_x = 10$. Both model integrated profiles were convolved with the spectrograph's instrumental profile, assuming its FWHM = 0.5 Å.

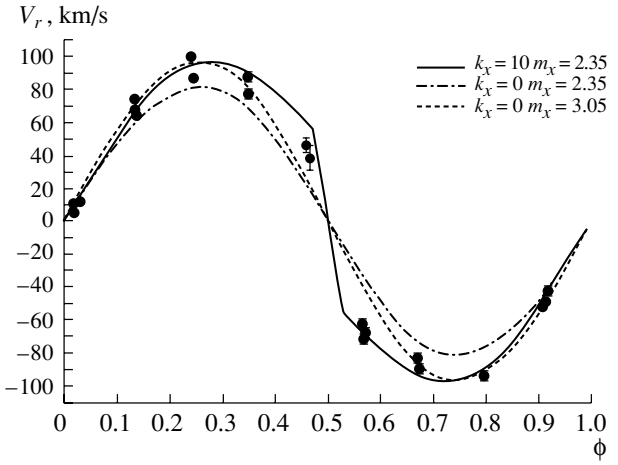

Fig. 4. Observed radial-velocity curve from [17] and the theoretical radial-velocity curves obtained for the Roche model with $i = 75°$. Shown are the best-fit radial-velocity curves for X-ray heating with $k_x = 10$, with $m_v = 2.4\,M_\odot$ and $m_x = 2.35\,M_\odot$ (solid); without X-ray heating ($k_x = 0$), with $m_v = 2.4\,M_\odot$ and $m_x = 2.35\,M_\odot$ (dash-dotted); and without X-ray heating ($k_x = 0$), with $m_v = 2.4\,M_\odot$ and $m_x = 3.05\,M_\odot$ (dashed). The other parameters of the binary are given in Table 1.

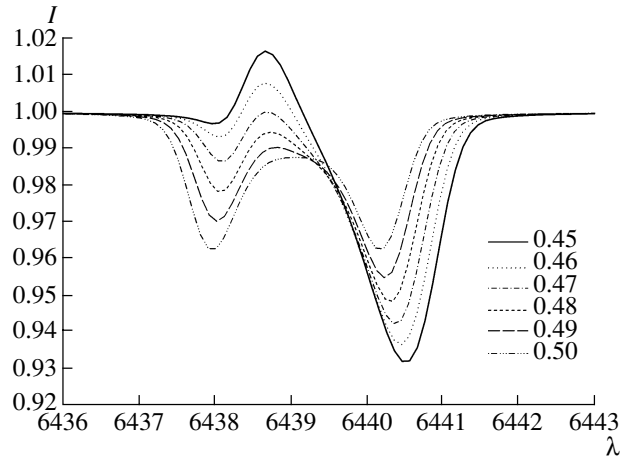

Fig. 5. Model integrated profiles of the CaI 6439 Å line obtained for the Roche model with X-ray heating of the optical component ($k_x = 10$) and for $m_v = 2.4\,M_\odot$, $m_x = 2.35\,M_\odot$, $i = 75°$. The other binary parameters are given in Table 1. Our notation for the orbital phases is shown near the curves.

scatter of the data points in the radial-velocity curve is probably due to variable X-ray heating of the star.

Let us compare the results of our fitting of the observed radial-velocity curve obtained using the Roche model with (Table 2) and without (Table 3) X-ray heating included. With X-ray heating ($k_x = 10$), with $i = 60°-90°$ and $m_v = 1.0-2.9\,M_\odot$, the mass of the relativistic object is found to be $m_x = 1.55-3.0\,M_\odot$; without X-ray heating ($k_x = 0$), the compact object's mass is found to be $m_x = 1.95-4.0\,M_\odot$. Thus, the fit of the data without X-ray heating of the optical star's atmosphere leads to masses of the compact object that are too high by $0.5-1.0\,M_\odot$.

Let us consider in more detail why m_x is systematically too high in the model without X-ray heating. Figure 3 displays the model integrated profiles of the CaI 6439 Å line at orbital phase $\phi = 0.25$ obtained for $m_v = 2.4\,M_\odot$, $m_x = 2.35\,M_\odot$, and $i = 75°$, with the X-ray heating taken (solid curve) and not taken (dashed curve) into account.

When the X-ray heating is taken into account, an emission component appears in the integrated profile of the absorption line (Fig. 3). Because of this emission component, the "center of gravity" of the absorption line is displaced. Thus, when the X-ray heating is included, the line's center of gravity in Fig. 3 is at a wavelength of 6441.131 Å, corresponding to a radial velocity of 95.44 km/s. If there is no X-ray heating, the line's center of gravity is at 6440.818 Å, corresponding to a radial velocity of 81.57 km/s. Thus, due to the distortion of the absorption line profile by the emission component, the observed amplitude of the optical component's radial-velocity curve can be explained using a lower mass for the compact object. For this reason, carefully taking into account the X-ray heating in the 2S 0921−63 binary reduces the compact object's mass from $m_x = 1.95-4.0\,M_\odot$ to $m_x = 1.55-3.0\,M_\odot$.

This is illustrated by the model radial-velocity curves in Fig. 4. For X-ray heating with $k_x = 10$, $m_v = 2.4\,M_\odot$, $i = 75°$, the minimum residual ($\chi^2_{\min} = 149.8$) is achieved for a mass of the compact object $m_x = 2.35\,M_\odot$ (solid curve in Fig. 4). The semiamplitude of the optical component's radial-velocity curve is $K_v = 96.81$ km/s. For the same binary parameters but without X-ray heating, the radial-velocity curve has a semiamplitude of $K_v = 81.27$ km/s (dash-dotted curve in Fig. 4). For the analysis without X-ray heating and with $m_v = 2.4\,M_\odot$ and $i = 75°$, the minimum residual ($\chi^2_{\min} = 356.7$) is achieved for the higher mass of the compact object $m_x = 3.05\,M_\odot$ (dashed curve in Fig. 4).

Let us also consider the shape of the optical star's absorption line in the presence of strong X-ray heating. It is obvious that estimates of the mass of the compact object depend directly on the uncertainty in the center of gravity of the absorption line in the optical star's spectrum. When analyzing the shape of model integrated profiles for the CaI 6439 Å line,

Table 4. Dependence of m_x on m_v for the Roche model with $i = 75°$, heating of the optical component with $k_x = 10$, and screening of the X-rays by the accretion disk

m_v, $M_\odot$	m_x, $M_\odot$
1.0	1.70
1.9	2.15
2.4	2.40
2.9	2.60

we encountered the problem of determining the line's center of gravity.

For example, in a binary with $m_v = 2.4\,M_\odot$, $m_x = 2.35\,M_\odot$, and $i = 75°$, the center of gravity of the line at phases 0.47−0.50 cannot be determined unambiguously. Figure 5 presents integrated profiles of the CaI 6439 Å line for orbital phases 0.45−0.50. We can see that, beginning with orbital phase 0.47, the line profile has two minima, preventing unambiguous determination of the center of gravity of the line, and hence of the radial velocity. For this reason, a break in the radial-velocity curve is observed at phases 0.47 and 0.53 (Fig. 4).

Because of the ambiguity in the absorption-line profiles in X-ray binary systems whose optical stars are heated, with $k_x \gtrsim 10$, it is difficult to derive a single satisfactory radial-velocity curve. Consequently, the masses of the relativistic objects must be estimated directly from the orbital variations of the observed line profiles, rather than from indirect data, such as radial-velocity curves. Modern 8−10-m telescopes can provide the needed high quality observational data for this purpose.

Model 2. Analysis of the Observed Radial-Velocity Curve with Screening of the X-ray Flux by the Accretion Disk

In this section, we allow for screening of the X-ray flux by the accretion disk, assuming the total screening angle of the accretion disk to be 5° [26] and the accretion disk to be situated in the binary's orbital plane. Some area elements on the optical star happen to be in the strip that is shielded from the X-rays from the relativistic object. We computed absorption-line intensities for these area proceeding as above, taking the local X-ray heating coefficient to be $k_x^{\rm loc} = 0$. We analyzed the observed radial-velocity curve for discrete masses of the optical star $m_v = 1.0$, 1.9, 2.4, and $2.9\,M_\odot$, and for $i = 75°$. The results are presented in Table 4.

Table 5. Dependence of the m_x on m_v for the Roche model with $k_x = 30$ and $i = 75°$

m_v, $M_\odot$	m_x, $M_\odot$	
	With screening of the X-rays	Without screening of the X-rays
1.0	1.65	1.60
1.9	2.08	2.05
2.4	2.30	2.28
2.9	2.50	2.45

The results were quite close to (for masses $m_v = 1.0\,M_\odot$ and $1.9\,M_\odot$, identical with) those obtained in the Roche model without screening of the X-ray flux by the accretion disk (Table 2). For this reason, we did not continue our analysis for orbital inclinations $i = 60°$ and 90°. The shadow strip on the optical component turned out to be too narrow to have any considerable influence on the results.

Similarly, we analyzed the observed radial-velocity curve allowing for screening of the X-ray flux by the accretion disk for the case $k_x = 30$, with $i = 75°$ and $m_v = 1.0$, 1.9, 2.4, $2.9\,M_\odot$, as in the previous case. The results are presented in Table 5. The derived masses are tabulated without error intervals because all the binary models were rejected at the 1 and 5% significance levels. The m_x values given correspond to the minimum χ^2 residuals.

It follows from Table 5 that including screening of the X-ray flux $L_x = 30\,L_v$ by the accretion disk has little influence on the results. The largest mass difference revealed for the two models is $0.05\,M_\odot$ (Table 5). The effect of screening will be even smaller if the heating coefficient is lower. Thus, the X-ray pulsar masses we derived earlier in [27] without allowing for screening of the X-ray flux by the accretion disks can be considered reliable.

Model 3. Analysis of the Observed Radial-Velocity Curve Allowing for Anisotropic X-ray Radiation from the Accretion Disk

To complete our study, we considered the hypothesis that the 2S 0921−630 binary contains a low-mass black hole. In this case, the X-rays from the accretion disk should be anisotropic, reducing the X-ray flux in the orbital plane. Note that the presence of strong emission components for many absorption lines in the optical component's spectrum [17] suggests that the X-ray radiation is isotropic. The emission lines in the

Table 6. Dependence of m_x on m_v for the Roche model with $k_x = 10$, anisotropic radiation from the X-ray source, and $i = 60°, 75°, 90°$

$m_v, M_\odot$	$m_x, M_\odot$		
	$i = 60°$	$i = 75°$	$i = 90°$
1.0	2.20	1.80	1.70
1.9	2.75	2.30	2.15
2.4	3.00	2.50	2.35
2.9	3.25	2.75	2.60

Table 7. Mass of the compact object in the 2S 0921−630 X-ray binary for various models, with $k_x = 10$

Model*	$m_x, M_\odot$
1	1.55–3.0
2	1.55–3.0
3	1.70–3.25

* Model 1: isotropic X-ray source, without screening of the X-ray flux by the accretion disk; model 2: isotropic X-ray source, with screening of the X-ray flux by the accretion disk; model 3: anisotropic X-ray source, without screening of the X-ray flux by the accretion disk.

spectrum of the optical star, which indicate considerable X-ray heating of the optical component, also provide indirect evidence that the system contains a neutron star.

We assumed the accretion disk to be optically thin and located in the binary's orbital plane. The anisotropy of the X-rays from the accretion disk was described with Eqs. (1) and (2) from [28]:

$$\frac{dL}{d\Omega} = \frac{L_x F(\theta)}{4\pi}, \qquad (1)$$

$$F(\theta) = \frac{6}{7}\cos\theta(1 + 2\cos\theta), \qquad (2)$$

where θ is the angle between the normal to the disk plane and the direction of an element of solid angle $d\Omega$. The geometry of the binary system for the Roche model with the parameters in Table 1 suggests that the X-ray flux falls on the optical component at $\theta \simeq 70°–90°$. We can see from (2) that the X-ray flux is considerably attenuated for such values of θ. Figure 6 presents the model integrated profiles of the CaI 6439 Å line at orbital phase 0.25. Note that the emission component of the integrated line profile is weaker than in the case of an isotropic X-ray flux.

The results of our fitting of the observed radial-velocity curve for the case of anisotropic X-rays from the accretion disk are presented in Table 6 and plotted in Fig. 7. We give the central values without uncertainties, since the binary models were rejected at the $\alpha = 1$ and 5% significance levels. For $m_v = 1.0–2.9\,M_\odot$, the mass of the black hole is $1.70–3.25\,M_\odot$. Recall that the compact object's mass for the case of isotropic X-rays with $k_x = 10$ was $m_x = 1.55–3.0\,M_\odot$. Thus, allowing for an anisotropic X-ray flux from the accretion disk

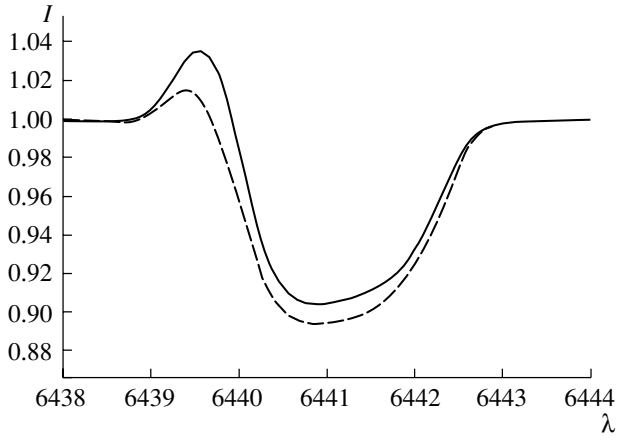

Fig. 6. Model integrated profiles of the CaI 6439 Å line of the optical component in the 2S 0921−630 X-ray binary system at orbital phase 0.25. The profiles were obtained for the Roche model with $m_x = 2.35\,M_\odot$, $m_v = 2.4\,M_\odot$, $i = 90°$, and $k_x = 10$. Shown are the absorption-line profile assuming isotropic (solid) and anisotropic (dashed) X-ray radiation from the compact object. Both model integrated profiles were convolved with the spectrograph's instrumental profile, assuming its FWHM = 0.5 Å.

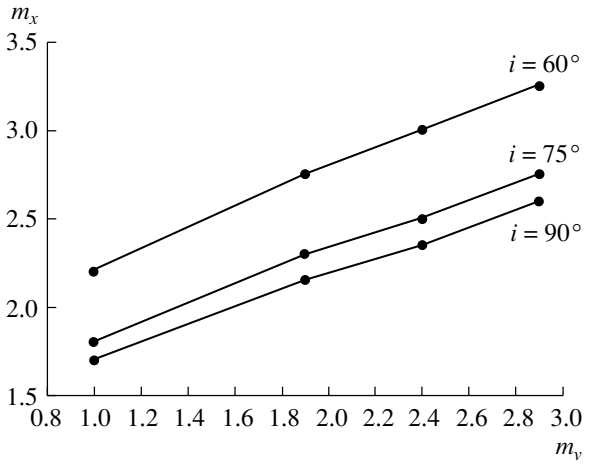

Fig. 7. Relation between the m_v and m_x in the 2S 0921−630 binary obtained by fitting the observed radial-velocity curve for the Roche model with $k_x = 10$ and anisotropic radiation from the accretion disk. See text for details.

increases the compact object's mass by $\sim 0.2\,M_\odot$ compared to the case of an isotropic X-ray flux.

4. DISCUSSION

The results of our analysis of the high-precision radial-velocity curve [17] (Fig. 1) with orbital inclinations $i = 60°-90°$ and the optical component's mass $m_v = 1.0-2.9\,M_\odot$ are presented in Table 7. We consider the mass of the compact object obtained in Model 1 to be our main result.

As we noted above, the binary exhibits X-ray eclipses, testifying to a high orbital inclination: $i \simeq 70°-90°$ [16]. Since there are no X-ray dips, we can assume $i > 80°$ [18]. For our mass estimates, we adopted values $i = 75°-90°$. In this case, assuming $m_v = 1.0-2.9\,M_\odot$, the mass of the compact object is $m_x \simeq 1.55-2.55\,M_\odot$ (Fig. 2). Taking into account the optical component's spectral type, K0III ($m_v \simeq 2.9\,M_\odot$ [29]), we find the compact object's mass to be $m_x = 2.45-2.55\,M_\odot$ (Fig. 2).

The actual mass of the optical star in an interacting binary, m_v, can differ from the estimate obtained based on its spectral type. For example, the mass estimates for the low-mass transient X-ray binaries V404 Cyg (spectral type of the optical star K0IV) and GRS 1915+105 (spectral type of the optical star KIII) derived from rotational broadening of absorption lines are $0.7 \pm 0.1\,M_\odot$ [30] and $0.81 \pm 0.53\,M_\odot$ [31], respectively. At the same time, the mass estimates based on the corresponding spectral types and luminosity classes are $\sim 1.3\,M_\odot$ and $\sim 2.3-2.9\,M_\odot$ [29], respectively. Thus, the estimates based on spectral type are too high by almost a factor of ~ 2 compared to the spectroscopic m_v values. This is in agreement with current theoretical ideas about stellar evolution in low-mass close binaries. According to computations using the "Scenario Machine" [11], an optical component with initial mass $\sim 3\,M_\odot$ loses more than $\sim 1\,M_\odot$ during the mass-exchange stage [12].

The optical stars in the X-ray binaries V404 Cyg, GRS 1915+105, and 2S 0921−630 have similar spectral types and luminosity classes [16, 31]. Assuming that the K0III star in the 2S 0921−630 system lost a substantial fraction of its mass via exchange and that its mass, like the optical star in GRS 1905+105, is $m_v \simeq 1\,M_\odot$, we find the mass of the compact object in the 2S 0921−630 system to be $m_x \simeq 1.6-1.7\,M_\odot$ (for $i = 75°-90°$). This is close to the mean mass of a neutron star, making it likely that we are dealing with an accreting neutron star in the 2S 0921−630 binary.

To extend our analysis for the 2S 0921−630 binary, we considered the possiblity that the compact object's mass is close to the standard mass of a neutron star, $m_x = 1.4\,M_\odot$. In this case, the mass of the optical component is $m_v = 0.65-0.75\,M_\odot$, where we have assumed $i = 75°-90°$ since partial X-ray eclipses are observed for the system [16]. Formally, from the stellar-evolution point of view, single stars with such masses cannot become giants over the Hubble time. In this case, the presence of a relativistic companion enables a star with an initial mass $\gtrsim 0.8\,M_\odot$ to lose some its mass during the semi-detached phase [32].

The result of the evolution of a giant with mass $\sim 0.6-0.7\,M_\odot$ is a helium white dwarf with mass $\sim 0.3-0.4\,M_\odot$ [32]. Thus, it is quite plausible that further evolution of the 2S 0921−630 X-ray binary will result in a millisecond radio pulsar in a binary with a helium white dwarf. This hypothesis is in a good quantitative agreement with the model computations of [32] and the empirical relation between the orbital periods and secondary (white dwarf) masses for binaries with millisecond radio pulsars (cf. [32, Fig. 4] and [33, Fig. 9]).

We note again that we rejected all models for the X-ray binary system at the $\alpha = 1$ and 5% significance levels. Tables 2–7 present the m_x values corresponding to the minimum χ^2 residuals. We must bear in mind that, in all cases, the models do not entirely adequately represent the observational data, so that our estimates of m_x cannot be considered final.

Note the importance of the methodological results of our study. Our computations for the Roche model demonstrated that the profile of the absorption line is rather complex in the case of strong X-ray heating, and suffers considerable variations in the course of the orbital motion (Figs. 3, 5). Thus, estimates of q based on rotational broadening of absorption-line profiles in low-mass X-ray binaries with strong X-ray heating cannot be considered trustworthy. Our future plans include a study of this problem.

5. CONCLUSIONS

Taking into account the large orbital inclination, $i = 75°-90°$, and our relations between the masses of the components in the 2S 0921−630 system (Fig. 2), we conclude that the mass of the compact object is $m_x \simeq 1.55-2.55\,M_\odot$ if the optical star's mass is $m_v = 1.0-2.9\,M_\odot$. Our study demonstrates that, if we allow for the possible mass loss by the optical component that reduces its mass to $m_v = 1\,M_\odot$, the presence of an accreting neutron star with $m_x \simeq 1.6-1.7\,M_\odot$ is most likely for this binary. The observed X-ray spectrum [24] of the compact object in 2S 0921−630 could correspond to a black hole, as well as to a neutron star with a weak magnetic field. It remains difficult to make an unambiguous selection between these possibilities for the nature of the compact object.

Our study demonstrates that high-resolution spectrograms ($\lambda/\Delta\lambda = 50\,000-100\,000$) are needed to estimate the compact object's mass. The most correct approach to estimating this mass, and hence revealing the nature of the compact object, is to fit the orbital variations of absorption-line profiles in the spectrum of the optical component.

ACKNOWLEDGMENTS

We thank A.V. Tutukov for helpful comments. This work was supported by the Russian Foundation for Basic Research (project no. 05-02-17489), the Program of Support for Leading Scientific Schools of Russia (NSh-388.2003.2), and a grant from the President of the Russian Federation (MK-2633.2005.2).

REFERENCES

1. S. E. Thorsett and D. Chakrabarty, Astrophys. J. **512**, 288 (1999).
2. A. G. Lyne, M. Burgay, M. Kramer, et al., Science **303**, 1153 (2004).
3. S. E. Woosley, A. Heger, and T. A. Weaver, Rev. Mod. Phys. **74**, 1015 (2000).
4. F. X. Timmes, S. E. Woosley, and T. A. Weaver, Astrophys. J. **457**, 834 (1996).
5. C. L. Fryer and V. Kalogera, Astrophys. J. **554**, 548 (2001).
6. P. Haensal, *EAS Publications Series,* Ed. by C. Motch and J.-M. Hameury (2003), Vol. 7, p. 249.
7. R. Ouyed and M. Butler, Astrophys. J. **522**, 453 (1999).
8. T. H. R. Skyrme, Proc. R. Soc. London, Ser. A **267**, 127 (1962).
9. R. Ouyed, Astron. Astrophys. **382**, 939 (2002).
10. R. Ouyed, astro-ph/0402122 (2004).
11. V. M. Lipunov, K. A. Postnov, and M. E. Prokhorov, *The Scenario Machine: Binary Star Population Synthesis,* Ed. by R. A. Sunyaev, Astrophys. Space Phys. Rev. **9** (Harwood, 1996).
12. A. I. Bogomazov, M. K. Abubekerov, V. M. Lipunov, and A. M. Cherepashchuk, Astron. Zh. **82**, 331 (2005) [Astron. Rep. **49**, 295 (2005)].
13. S. B. Popov and M. E. Prokhorov, Astron. Astrophys. **434**, 649 (2005).
14. F. K. Li, G. W. Clark, J. G. Jernigan, et al., Nature **276**, 799 (1978).
15. G. Branduardi-Raymont, R. H. D. Corbert, K. O. Mason, et al., Mon. Not. R. Astron. Soc. **205**, 403 (1983).
16. T. Shahbaz, E. Kuulkers, P. A. Charles, et al., Astron. Astrophys. **344**, 101 (1999).
17. P. G. Jonker, D. Steegh, G. Nelemans, and M. van der Klis, Mon. Not. R. Astron. Soc. **356**, 621 (2005).
18. J. Frank, A. R. King, and J.-P. Lasota, Astron. Astrophys. **178**, 137 (1987).
19. R. A. Wade and K. Horne, Astrophys. J. **324**, 411 (1988).
20. E. A. Antokhina and A. M. Cherepashchuk, Astron. Zh. **71**, 420 (1994) [Astron. Rep. **38**, 367 (1994)].
21. E. A. Antokhina, Astron. Zh. **73**, 532 (1996) [Astron. Rep. **40**, 483 (1996)].
22. E. A. Antokhina, A. M. Cherepashchuk, and V. V. Shimanskii, Izv. Ross. Akad. Nauk, Ser. Fiz. **67** (3), 293 (2003).
23. E. A. Antokhina, A. M. Cherepashchuk, and V. V. Shimanskii, Astron. Zh. **82**, 131 (2005) [Astron. Rep. **49**, 109 (2005)].
24. T. R. Kallman, L. Angelini, B. Boroson, and J. Cottam, Astrophys. J. **583**, 861 (2003).
25. A. M. Cherepashchuk, Astron. Zh. **70**, 1157 (1993) [Astron. Rep. **37**, 585 (1993)].
26. N. I. Shakura and R. A. Sunyaev, Astron. Astrophys. **24**, 337 (1973).
27. M. K. Abubekerov, E. A. Antokhina, and A. M. Cherepashchuk, Astron. Zh. **81**, 108 (2004) [Astron. Rep. **48**, 89 (2004)].
28. N. G. Bochkarev, R. A. Syunyaev, T. S. Khruzina, et al., Astron. Zh. **65**, 778 (1988) [Sov. Astron. **32**, 405 (1988)].
29. V. Straizhis, *Metal-Deficient Stars* (Mokslas, Vilnius, 1982) [in Russian].
30. J. Casares and P. A. Charles, Mon. Not. R. Astron. Soc. **271**, L5 (1994).
31. E. T. Harlaftis and J. Greiner, Astron. Astrophys. **414**, L13 (2004).
32. A. V. Tutukov and A. V. Fedorov, Astron. Zh. **80**, 652 (2003) [Astron. Rep. **47**, 637 (2003)].
33. D. R. Lorimer, astro-ph/0511258 (2005).

Translated by N. Samus'